Investigation of the effects of the platform motion on the aerodynamics of a floating offshore wind turbine

Yuan-chuan Liu[1], Qing Xiao[1*], Atilla Incecik[1] and De-cheng Wan[2]

1. *Department of Naval Architecture, Ocean and Marine Engineering, University of Strathclyde, Glasgow, G4 0LZ, UK*
2. *State Key Laboratory of Ocean Engineering, School of Naval Architecture, Ocean and Civil Engineering, Shanghai Jiao Tong University, Shanghai, 200240, China*

Abstract: Along with the flourishing of the wind energy industry, floating offshore wind turbines have aroused much interest among the academia as well as enterprises. In this paper, the effects of the supporting platform motion on the aerodynamics of a wind turbine are studied using the open source CFD framework OpenFOAM where the platform motion responses, including surge, heave and pitch, are superimposed onto the rotation of the wind turbine. Thrust and torque on the wind turbine are compared and analysed for cases under different platform motion patterns, together with the flow field. It is shown that the movement of the supporting platform can have large influences on a floating offshore wind turbine and need be considered during the design process.

Keywords: floating offshore wind turbine; superimposed platform motion; aerodynamics; OpenFOAM

1 Introduction

Over the last few decades, wind energy has been widely adopted as a clean and renewable energy source. According to a report published by the European Wind Energy Association (EWEA, 2014), the share of renewable energy in total new power capacity installations in the European Union has grown from 22.4% to 72% during 2000 and 2013. Of all 385 GW of new power capacity installations in the EU since 2000, over 28% has been wind power. While offshore wind business is growing rapidly, a lot of research institutions and companies are now busy developing and designing new generation floating offshore wind turbines which will be installed in deep water areas (DeepCwind, 2013; FORWARD, 2013; Quallen et al., 2014; Tran and Kim, 2015). The reasons and advantages of floating wind turbines in deep water areas are: shallow water sites for fixed wind turbines are limited; wind far off the coast is even more abundant; public concern about visual impacts caused by turbines can be minimized.

Unlike its fixed counterpart, a floating wind turbine must be supported by a floating platform which, however, further complicates the design process. The upper turbine and the lower supporting platform are coupled in one way or another. Thrust and torque acting on the turbine are added to the motion equation system of the platform while the movement of the latter also affects the position and orientation of the former thus its aerodynamic performance. Much research on the aerodynamic analysis for a floating wind turbine under the influence of the platform motion has been done by decoupling the movement of the platform from the system as a simplification. Jeon et al. (2014) adopted a vortex method to simulate a floating wind turbine undergoing prescribed pitch motion. It was shown that when the platform moves in the upward direction to the position with highest velocity, thrust becomes largest as well due to the largest relative velocity. Effects of induced velocity were also studied. de Vaal et al. (2014) studied a floating wind turbine with prescribed surge motion using the BEM method with various dynamic wake models as well as the actuator disk method. It was shown that the integrated rotor loads were almost the same for all methods, indicating that current engineering models for wake dynamics seem to be sufficiently capable of dealing with the additional unsteady surge motion of a wind turbine rotor in a global force analysis. Tran and Kim (2015) and Tran et al. (2014) used commercial CFD packages to study the aerodynamic performance of a FOWT experiencing platform pitching motion. Results were compared with those from other simplified models. Aerodynamic loads of the blade were demonstrated to change drastically with respect to the frequency and amplitude of platform pitching motion.

Most of the research work has focused on prescribing a single degree of freedom (DoF) for the platform. However, from the perspective of a floating structure, among the all 6DoF motion responses, surge, heave and pitch are usually present at the same time. By taking these three degrees of freedom into consideration simultaneously, a more realistic representation for the movement of the supporting platform could be made and the effects of the platform motion on the aerodynamic performance of a floating wind turbine could be better illustrated. In this paper, the open source CFD framework known as OpenFOAM (OpenFOAM, 2015) is adopted to study the effects of the supporting platform motion on the aerodynamics of a wind turbine. The platform motion responses, including surge, heave and pitch, are superimposed onto the rotation of the wind turbine.

2 Methodology

In the present study, the pimpleDyMFoam solver in OpenFOAM is used which is suitable for solving transient, incompressible and single-phase flow of Newtonian fluids with the moving mesh capability (OpenFOAM, 2015). The incompressible Reynolds-averaged Navier-Stokes (RANS) equations with the k-ω SST turbulence model are discretised using the Finite Volume Method (FVM). The PIMPLE

***Corresponding author Email:** qing.xiao@strath.ac.uk

(merged PISO-SIMPLE) algorithm is applied to deal with the velocity-pressure coupling in a segregated way. A second-order backward scheme is used for the temporal discretisation and a second-order upwind scheme is applied for the convective term.

OpenFOAM implemented a sliding mesh technique called Arbitrary Mesh Interface (AMI) for rotating machinery problems (OpenFOAM, 2011), which allows simulation across disconnected, but adjacent, mesh domains either stationary or moving relative to one another. And AMI is adopted in this study for the rotation of wind turbine. The prescribed surge, heave and pitch motion responses are applied to the whole computational domain including the rotor domain in such a way that the position and rotation of the turbine rotor are determined by the superimposed motion of its own rotation and the 3DoF platform movement.

3 Computational Model

3.1 Geometry

The NREL Phase VI wind turbine is used in this study. Although this model was initially designed for the application under onshore scenarios, the availability of experimental data (Hand et al., 2001) from the National Renewable Energy Laboratory (NREL) makes it a popular validation case for codes studying aerodynamic performance of wind turbines. As a result, this model is used for validation first and then as a base model for cases with prescribed platform motion.

The NREL Phase VI wind turbine is a two-blade upwind model and each blade uses the NREL S809 airfoil profile shown in Fig. 1 at most of its span wise cross sections. The length of the blade is 5.029 m from tip to the rotation axis. Of all the configurations tested by NREL, a tip pitch angle of 3 degrees is used and zero yaw angle is applied. A CAD model for the wind turbine is shown in Fig. 2. The hub, nacelle and tower are not considered here for simplicity. Detailed geometry parameters can be found in the NREL report (Hand et al., 2001).

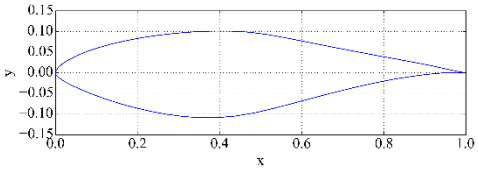

Fig. 1 Profile of NREL S809 airfoil

Fig. 2 CAD model of NREL Phase VI wind turbine

3.2 Computational Mesh

The overall computational domain is a large cylinder shown in Fig. 3 with a diameter of 5D where D stands for the diameter of the rotor. The inlet and outlet boundaries are 1.5D and 4D away from the rotor respectively. The rotor is surrounded by a smaller cylinder region and the faces connecting the two cylinder regions are defined as the AMI sliding interface. For a fixed wind turbine simulation, the inner smaller cylinder region (or rotor region) will rotate about a predefined axis while the outer domain (or stator region) will maintain static.

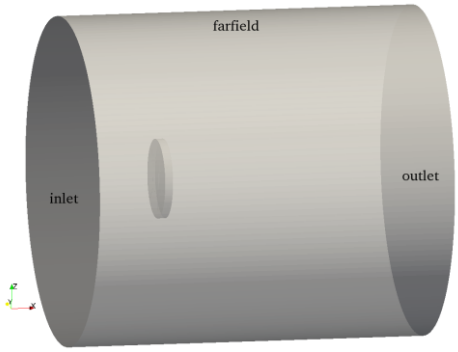

Fig. 3 Overall computational domain

A hybrid meshing technique is adopted. Inside the rotor region, an unstructured mesh is used due to the complexity of the rotor geometry, while a multi-block structured mesh topology is applied for the outer stator region. An illustration of the overall computational mesh can be seen in Fig. 4. Detailed mesh is also shown in Fig. 5.

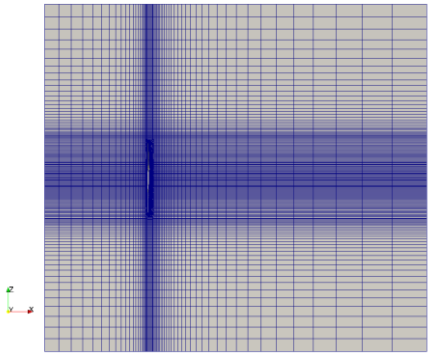

Fig. 4 Overall computational mesh

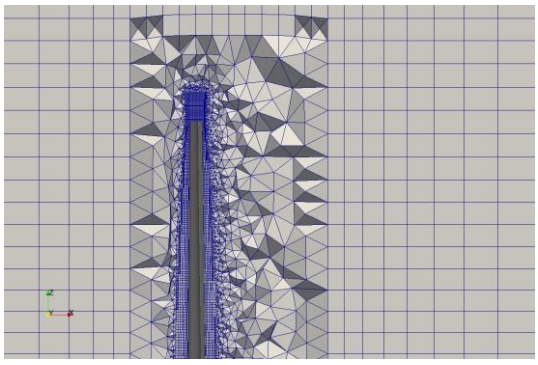

(a) Near rotor region

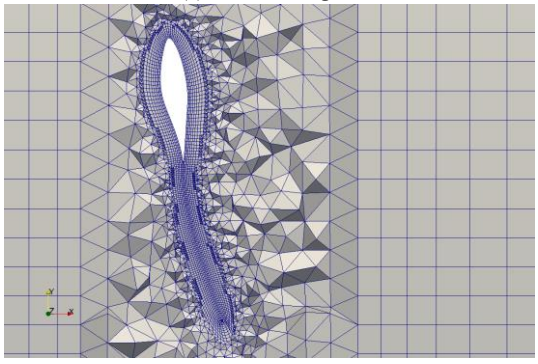

(b) Sectional view

Fig. 5 Detailed mesh

Since the k-ω SST turbulence model implemented in OpenFOAM is a high-Reynolds model, wall functions are used at the rotor boundary for k and ω variables. A spacing of 0.0045 m is applied for near wall grid cells to make sure the y+ value lies inside the interval of [30, 300]. Ten layers of boundary layer cells are added near the rotor boundary to better capture the fluid flow near the rotor. The overall computational grid size is about 5.8 M.

4 Validation

Validation is first done for the originally fixed wind turbine model. Four different wind velocities (5, 10, 15 and 25 m/s) are investigated and the rotational speed is constantly fixed at 72 RPM.

4.1 Thrust and Torque

Thrust and torque are two of the most important aerodynamic performance parameters for a wind turbine. They represent the integrated loading on the turbine. Due to unsteadiness caused by flow turbulence, both thrust and torque vary with regards to time. The results presented here are obtained by averaging the time history curves over a certain period of time. A comparison between the present results and data obtained from the NREL report (Hand et al., 2001) is demonstrated in Fig. 6. The vertical bars in the figures represent the experimental standard deviation.

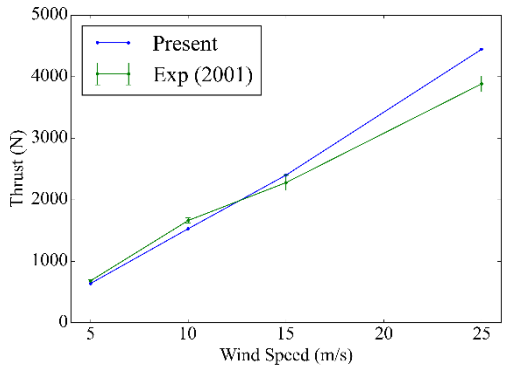

(a) Thrust

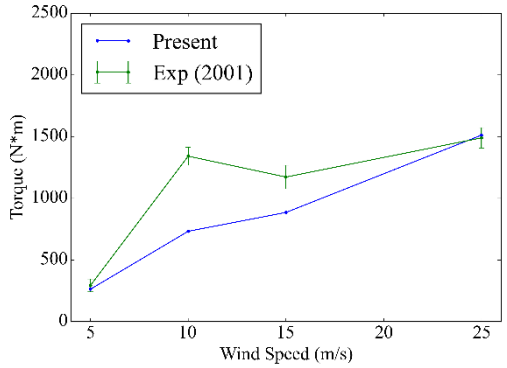

(b) Torque

Fig. 6 Comparison of thrust and torque

The difference between the predicted thrust and experimental data is acceptable. However, the present simulation under-predicts the torque value for the cases with a wind speed of 10 and 15 m/s. The underestimation might be attributed to the fact that these two wind speeds are closer to the stall point (Sørensen et al., 2002) and a finer grid resolution might be needed to achieve better agreement.

4.2 Pressure Coefficients

Pressure coefficients can reflect local and more detailed flow information than thrust and torque, and is defined here as:

$$C_p = \frac{P_0 - P_\infty}{0.5\rho\left[U^2 + (\omega r)^2\right]} \quad (1)$$

where P_0 and P_∞ are the measured pressure at a given location and the reference pressure in the farfield; U stands for the wind velocity; ω is the rotational speed and r denotes the distance between the section and rotation centre.

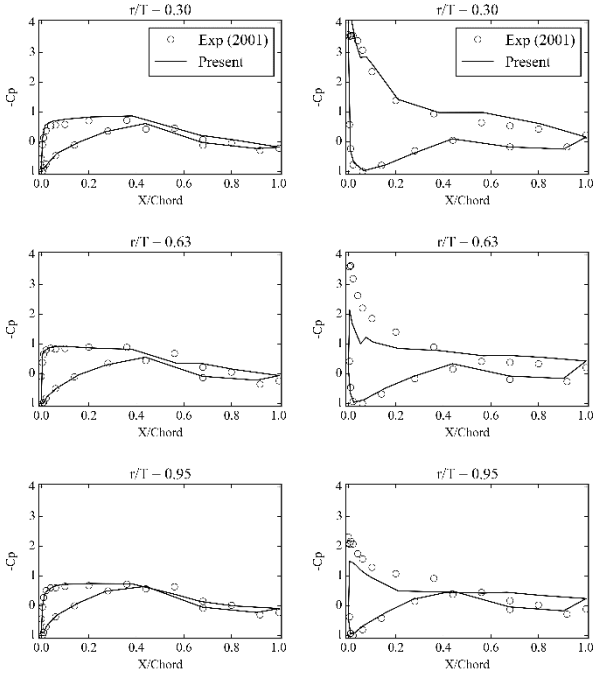

(a) U = 5 m/s (b) U = 10 m/s

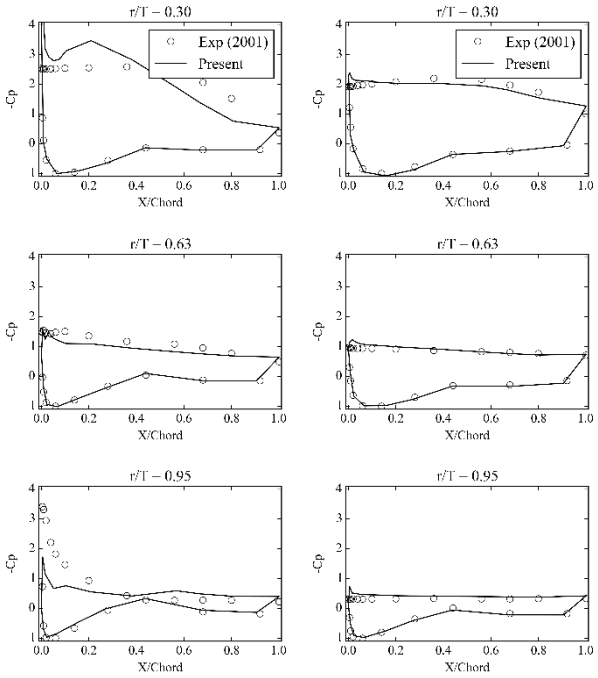

(c) U = 15 m/s (d) U = 25 m/s

Fig. 7 Pressure coefficient for different velocities

Fig. 7 shows the comparison between predicted and measured pressure coefficients at three cross sections for four different wind velocities. At 5 m/s and 25 m/s, results from simulation agree well with those from experimental tests; for all four wind velocities, good agreement can also be achieved for the pressure coefficients on the pressure side of the blade (lower part of the curves). The discrepancies for the pressure coefficients on the suction side (upper part of the curves) at 10 m/s and 15 m/s can partly explain the underestimation of torque for these two cases. The present simulation fails to capture the peak pressure near the leading edge, especially at r/R = 0.63 and 0.95.

5 Working Conditions

To investigate the effects of platform motion on the aerodynamic performance of the wind turbine, prescribed 3DoF platform motion responses (surge, heave and pitch) are superimposed in a sinusoidal form onto the rotation of the turbine rotor. Since the wind turbine was originally designed for onshore applications, assumptions need be made if platform motion is to be considered.

Offshore wind turbines usually have larger rotor diameters than onshore turbines. In the present study, the investigated turbine is assumed to be the 1:16 scaled model of a real offshore floating wind turbine with a blade length of about 80 m. The surge, heave and pitch amplitudes are estimated based on the 1:16 scale ratio as 0.25 m, 0.1 m and 2 ° separately. The centre of platform pitch motion is 6 m away in the z direction from the centre of rotation for the turbine rotor. Under regular wave conditions, the motion period for all three DoF's is the same as the incoming wave period. Four different values for the motion period are applied to investigate its influence, which are listed in Table 1. The Froude scaling law is used to determine the periods in model scale. For all cases, the wind velocity is kept as 15 m/s.

Table 1 Working conditions

Case No.	1	2	3	4
Motion Period (s)-full scale	10	4.8	3.33	2.4
Motion Period (s)-model scale	2.5	1.2	0.833	0.6

6 Results and Discussion

6.1 Thrust and Torque

Fig. 8 depicts the thrust and torque time history curves under different motion periods. It can be seen that both thrust and torque are largely affected by the superimposition of the platform motion. In fact, the smaller the motion period is, the larger the amplitudes for thrust and torque are. And the mean values are still the same as those in fixed conditions. Take motion period T = 0.6 s for example, the maximum thrust is almost 40% higher than the mean value while the minimum thrust is about 40% lower. Considering the large difference between the extrema, fatigue will need be taken into account over the design process. Variance of torque will also directly influence the power generated by the turbine with regard to time.

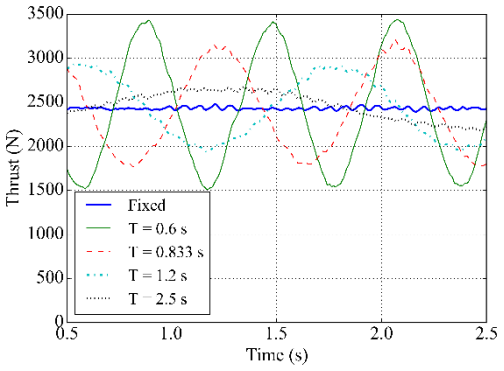

(a) Thrust

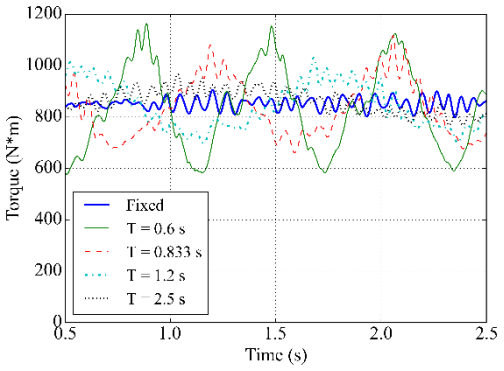

(b) Torque

Fig. 8 Comparison of thrust and torque under various motion periods

6.2 Flow Filed

Prescribed platform motion also influences the flow field. Take motion period T = 1.2 s for example, Fig. 9 demonstrates the pressure distribution near the turbine rotor for four instances. A slice is made at y = 0 in the beginning and rotates along with the turbine.

(a) Time = 1.2 s

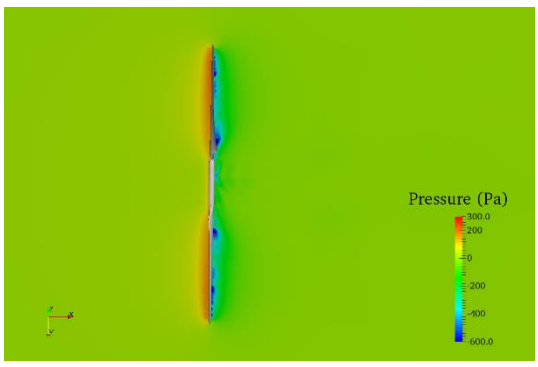

(b) Time = 1.5 s

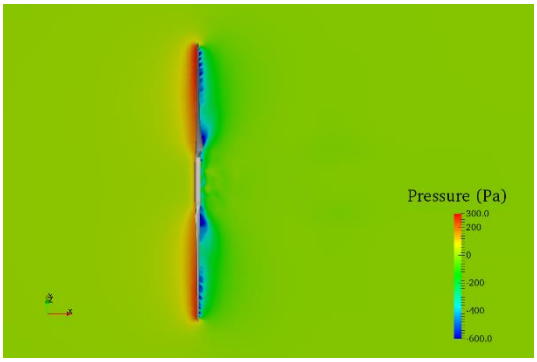

(c) Time = 1.8 s

(d) Time = 2.1 s

Fig. 9 Instantaneous pressure distribution near turbine rotor

Fig. 10 shows the prescribed motion with regard to time over one period. At 1.2 s, motion is zero but velocity is at its maximum. For surge motion, it means that the surge velocity is in the same direction as the wind velocity, reducing the relative wind velocity. The pressure difference as shown in Fig. 9 before and after the rotor is small, which corresponds to the minimum thrust in Fig. 8. At 1.5 s, although motion is at its maximum, velocity becomes zero just as in the case without prescribed platform motion. The thrust at this instance is very close to the value with a fixed wind turbine as shown in Fig. 8. The pressure difference becomes larger, so is the thrust. At 1.8 s, surge velocity reaches its maximum in the direction opposite to the wind velocity, making the relative wind velocity largest. The large pressure distribution in Fig. 9 indicates the maximum thrust in Fig. 8. Situation at 2.1 s is very similar to that at 1.5 s.

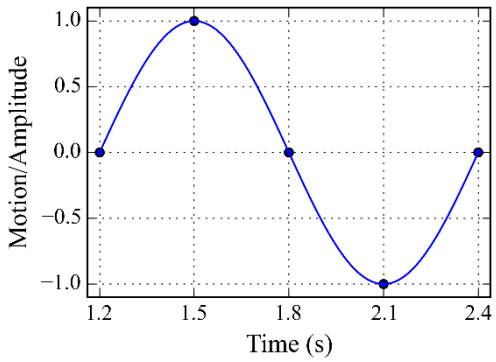

Fig. 10 Motion curve with regard to time

Fig. 11 shows the vortices using the iso-surface of the second invariant of the rate of strain tensor (Q) at Q = 5. Strong vortices can be seen at blade tips as well as the blade root where the geometry quickly changes from the NREL S809 airfoil profile to cylindrical sections. The vertical structure is also clearly influenced by the prescribed platform movement. When the turbine moves in the wind direction, it will interfere with its own wake, resulting in the disappearing of vortices as can be seen in Fig. 11 (a~b). When the turbine moves in the direction opposite to the wind velocity, vortices increase again as shown in Fig. 11 (c~d).

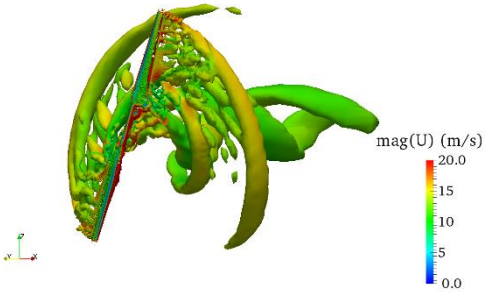

(a) Time = 1.2 s

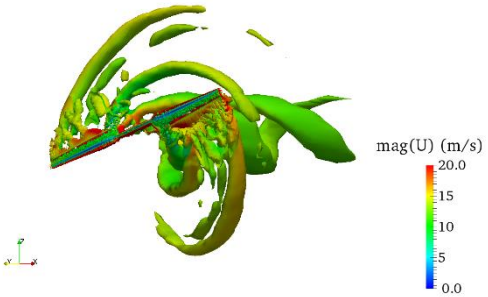

(b) Time = 1.5 s

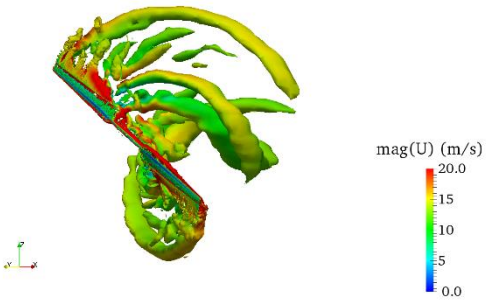

(c) Time = 1.8 s

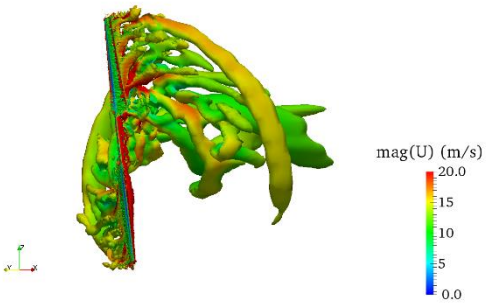

(d) Time = 2.1 s

Fig. 11 Instantaneous vortices visualisation (Q = 5) coloured by velocity magnitude

7 Conclusions

In this paper, an open source CFD solver was applied to perform aerodynamic simulation for the NREL Phase VI wind turbine model. Validation was first done against experimental test under fixed conditions. Numerical experimentation was later carried out by superimposing the prescribed platform 3DoF motion (surge, heave and pitch) onto the rotation of the wind turbine to simulate a floating wind turbine moving along with the supporting platform. Various motion periods were tested and aerodynamic thrust and torque of the wind turbine were compared. It was found that both thrust and torque would be largely influenced by the prescribed platform motion, indicating that the motion response of the supporting platform for a floating wind turbine should be taken into account during the design process. Fluid field variables such as pressure and vortices were also visualised and analysed. In the next step, the motion response of the platform would be computed due to both wave and wind loading rather than prescribed to better represent working conditions.

Acknowledgement

Results were obtained using the EPSRC funded ARCHIE-WeSt High Performance Computer (www.archie-west.ac.uk). EPSRC grant no. EP/K000586/1. This work also used the ARCHER UK National Supercomputing Service (http://www.archer.ac.uk).

References

de Vaal JB, Hansen MOL, Moan T (2014). Effect of wind turbine surge motion on rotor thrust and induced velocity. *Wind Energy*, **17**(1), 105-121.

DeepCwind. 2013. Available from: http://www.deepcwind.org/.

EWEA. Wind in power: 2013 European statistics. 2014: 12.

FORWARD F. 2013. Available from: http://www.fukushima-forward.jp/english/.

Hand MM, Simms D, Fingersh L, Jager D, Cotrell J, Schreck S, Larwood S. Unsteady aerodynamics experiment phase VI: wind tunnel test configurations and available data campaigns. 2001.

Jeon M, Lee S, Lee S (2014). Unsteady aerodynamics of offshore floating wind turbines in platform pitching motion using vortex lattice method. *Renewable Energy*, **65**, 207-212.

OpenFOAM. Arbitrary Mesh Interface (AMI). 2011. Available from: http://www.openfoam.org/version2.1.0/ami.php.

OpenFOAM. The OpenFOAM website. 2015. Available from: http://www.openfoam.com/.

Quallen S, Xing T, Carrica P, Li Y, Xu J (2014). CFD Simulation of a Floating Offshore Wind Turbine System Using a Quasi-static Crowfoot Mooring-Line Model. *Journal of Ocean and Wind Energy*, **1**(3), 143-152.

Sørensen NN, Michelsen JA, Schreck S (2002). Navier–Stokes predictions of the NREL phase VI rotor in the NASA Ames 80 ft × 120 ft wind tunnel. *Wind Energy*, **5**(2-3), 151-169.

Tran T-T, Kim D-H (2015). The platform pitching motion of floating offshore wind turbine: A preliminary unsteady aerodynamic analysis. *Journal of Wind Engineering and Industrial Aerodynamics*, **142**(0), 65-81.

Tran T, Kim D, Song J (2014). Computational Fluid Dynamic Analysis of a Floating Offshore Wind Turbine Experiencing Platform Pitching Motion. *Energies*, **7**(8), 5011-5026.